Variations in reflectance with seasonality and viewing geometry: Implications for classification of Brazilian savanna physiognomies with MISR/Terra data

Veraldo Liesenberg, Lênio Soares Galvão *, Flávio Jorge Ponzoni

Instituto Nacional de Pesquisas Espaciais (INPE), Divisão de Sensoriamento Remoto, Av. dos Astronautas, 1758, Bairro Jardim da Granja, Caixa Postal 515, 12245-970, São José dos Campos, SP, Brasil

Abstract

Bidirectional Reflectance Factor (BRF) data, collected at nine view angles, four bands and six dates by the Multi-angle Imaging SpectroRadiometer (MISR), were used to characterize the seasonality and viewing geometry effects on the discrimination of five selected physiognomies of a specific Brazilian savanna environment. Spectral–angular profiles for each physiognomy (Seasonal, Dry and Pluvial Forests; Arboreous and Park Savanna) were obtained from nadir-normalized BRF data at each MISR band and date of image acquisition. The maximum likelihood classification technique was applied at each camera and date using a common set of pixels as training samples. A reference map was used as ground truth to obtain the classification accuracy for each physiognomy, view angle and date. Results showed that the surface anisotropy signatures of the savanna physiognomies were not unique and varied with Sun-view geometry and seasonality. Directional effects increased from data collected in the orthogonal plane to those acquired close to the solar principal plane, and with increasing Sun zenith angles. Such effects were also affected by seasonality due to differences in the dynamics of the vegetation response to precipitation, as indicated by the Fraction of Photosynthetically Active Radiation (FPAR) and Leaf Area Index (LAI) values. Dry Forest presented a faster rate of "green-up" in the beginning of the rainy season and more abrupt changes in LAI values earlier in the dry season than the other physiognomies. In relation to the nadir response, the strongest anisotropy was observed in the backward scattering direction and in the red band at large Sun zenith angles. Directional effects were also observed after the Normalized Difference Vegetation Index (NDVI) determination. Classification accuracy of vegetation improved from the rainy to the dry season. The exception was Park Savanna, which was also well discriminated from the other physiognomies in the beginning of the rainy season due to the spectral effects of non-photosynthetic vegetation (dry grass understore) that produced an increase in the red reflectance. In general, classification accuracy of the physiognomies improved also from the forward to the backward scattering direction. The best view angles for classification purposes ranged from 0° (nadir) to −45.6°, and were associated with viewing directions of maximum backscattering at the different dates. In comparison with single view direction results, the use of Anisotropy Index (ANIX) images produced a general decrease in classification accuracy values. Results indicated that off-nadir viewing can improve discrimination and mapping of major physiognomies in the Brazilian savanna environment.
© 2006 Elsevier Inc. All rights reserved.

Keywords: MISR; Savanna; Classification; *Cerrado*; View angle; Sun zenith; Seasonality

1. Introduction

The Brazilian tropical savanna, locally known as "*Cerrado*", is the second largest biome of this country, after the Amazon forest. It presents unique and rich biodiversity and consists of small trees scattered and interspersed by shrubs and grasses in variable proportions (Oliveira-Filho & Ratter, 2002; Ribeiro & Walter, 1998; Silva & Bates, 2002). This biome shows plant species well adapted to fire and to the strong seasonal contrast observed in precipitation between the dry and rainy seasons (Eiten, 1982; Gillon, 1983; Sarmiento, 1983). It has been rapidly converted into pasture and agricultural areas (Jepson, 2005; Sano et al., 2001). According to Ratana et al. (2005), remote sensing provides useful information to monitor the Brazilian savanna physiognomies and to analyze their seasonal
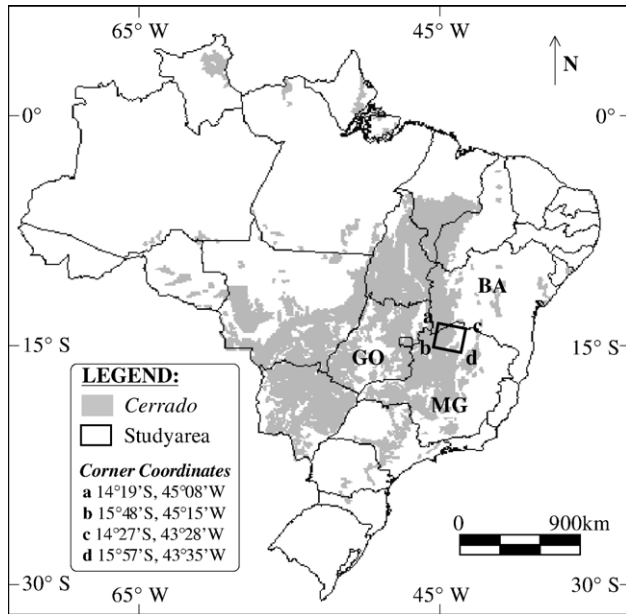

Fig. 1. Location of the study area in the States of Minas Gerais (MG) and Bahia (BA) close to the limits of the State of Goiás (GO). The spatial distribution of the Brazilian savannas (Cerrado) is also illustrated.

discrimination from multi-view angle observations, a better understanding of how sunlight is scattered at distinct view angles by the savanna physiognomies is still necessary.

In this article, variations in Bidirectional Reflectance Factor (BRF) (MISR Level 2 Land Surface Data) of five major physiognomies of a Brazilian savanna environment are analyzed as a function of the viewing geometry and seasonality. To demonstrate the seasonality and Sun-view angle effects on the discrimination of these selected physiognomies, MISR data (1.1 km of spatial resolution) collected in the rainy and dry seasons at nine view angles and six dates are evaluated for classification purposes.

2. The study area

The study area is located in the States of Minas Gerais and Bahia close to the limits of the State of Goiás (Fig. 1). The climate is tropical with monthly average temperatures above 24 °C. The study area shows well-defined rainy (November to April) and dry (May to October) seasons with annual average precipitation of 925 mm. More than 85% of precipitation frequently occurs between November and March. In some portions of the study area, the original vegetation cover has been rapidly converted into agricultural areas.

Five major physiognomies occur in the savanna environment of the study area. According to the Brazilian system of vegetation classification (IBGE, 1992), the physiognomies are: Floresta Estacional Semi-Decidual (henceforth named Seasonal Forest), Floresta Estacional Decidual (Dry Forest), Floresta Pluvial (Pluvial Forest), Savana Arborizada (Arboreous Savanna) and Savana Parque (Park Savanna). In the savanna classification system proposed by Ribeiro and Walter (1998), the physiognomies Arboreous Savanna and Park Savanna of the study area are equivalent to the Cerrado stricto sensu (Savanna Woodland) and Cerrado Ralo (Wooded Savanna), respectively. The percentage of trees that drop their leaves in the dry season ranges from 20% to 50% for Seasonal Forest, and is more than 50% for Dry Forest. Pluvial Forest occurs in the flooded plain areas. Arboreous Savanna and Park Savanna present both small palms, shrubs, twisted or leaning trees over a grass understore. However, Arboreous Savanna shows a more woody-dominated stratum and a closer canopy cover than Park Savanna.

To give a better idea on the differences between the physiognomies in the study area, Table 1 presents vegetation parameters measured in fieldwork activities on 38 representative sample plots. Canopy cover of woody species, calculated from the vertical projection of their outermost perimeter, decreased from the

patterns and dynamics. Examples of the use of spectral vegetation indices to discriminate these physiognomies were given by Ferreira et al. (2004), Ferreira and Huete (2004) and Sano et al. (2005).

The ability of the Multi-angle Imaging SpectroRadiometer (MISR) on-board the Terra satellite to obtain quasi-simultaneous multi-spectral measurements at nine view angles has provided unique information for mapping vegetation and quantifying canopy structure and photosynthetic activity (Braswell et al., 2003; Diner et al., 1999, 2005; Gobron et al., 2002; Hu et al., 2003; Lotsch et al., 2003; Nolin, 2004; Zhang et al., 2002). In general, changes produced in sensor signal due to off-nadir viewing are dependent on the geometry of data acquisition, the wavelength and on the vegetation type under study (Asner et al., 1998; Galvão et al., 2004; Kimes et al., 1984, 1994; Leroy & Roujean, 1994; Verbrugghe & Cierniewski, 1995; Walther-Shea et al., 1997). Such changes may be useful to improve classification accuracy of the land cover classes (Abuelgasim et al., 1996; Sandmeier & Deering, 1999; Xavier & Galvão, 2005). In relation to nadir measurements, off-nadir viewing may provide an additional source of information to discriminate the Brazilian savanna physiognomies because of the anisotropy of their reflectance distribution that may also change with both seasonality and Sun zenith angle. To optimize their

Table 1
Average and standard deviation values of vegetation parameters measured in the rainy season for the five physiognomies under study

Physiognomies	Canopy cover (%)	Basal area (m²/ha)	DBH (cm)	Tree height (m)	Crown diameter (m)	Number of trees per ha
Seasonal Forest	72.11±21.93	55.0±16	14.20±0.84	6.11±1.78	2.93±1.36	1475±515
Dry Forest	61.79±16.33	62.5±13	8.78±4.32	4.25±1.84	2.43±1.33	3222±1360
Arboreous Savanna	46.57±14.92	53.0±12	11.55±4.49	4.80±2.07	3.13±2.35	1454±552
Pluvial Forest	41.29±23.77	88.0±14	5.81±1.16	4.67±0.36	1.02±0.40	3063±398
Park Savanna	30.99±10.44	37.0±12	9.13±1.28	2.99±0.75	1.44±0.34	1620±757

DBH is the tree diameter at breast height.

Seasonal and Dry Forests to the remaining physiognomies. Pluvial Forest presented the largest value of basal area (the cross section area of the stems of the plants) whereas Park Savanna showed the lowest value of tree height. DBH (tree diameter at breast height) and crown diameter values decreased from Seasonal Forest and Arboreous Savanna to the other physiognomies. Finally, the greatest proportion of trees was measured for the Dry and Pluvial Forests. In the dry season, the Seasonal Forest and especially Dry Forest presented strong leaf fall in the study area, as mentioned before. Furthermore, non-photosynthetic vegetation (dry grass, leaf litter, and woody material) became also a very important spectral component of the other physiognomies.

Variations in vegetation parameters of Table 1 are consistent with values of the vegetation continuous field product (Hansen et al., 2002) from the Moderate Resolution Imaging Spectroradiometer (MODIS) for pixels approximately equivalent to the sampled plots. According to this dataset, tree cover decreased from the Seasonal and Dry Forests to the Arboreous Savanna, Pluvial Forest and Park Savanna which presented the greatest proportion of herbaceous cover. Bare cover was observed only in the Arboreous Savanna and Park Savanna areas and presented small values.

3. Methodology

3.1. MISR data acquisition

MISR BRF data (Level 2 Land Surface Data; version LAND F04-0015) with 1.1 km of spatial resolution were obtained at six dates to represent a seasonal cycle: November 17, 2003 (beginning of the rainy season); April 25, 2004 (end of the rainy season); June 28, July 30, August 15, 2004 (dry season); and October 02, 2004 (end of the dry season). In fact, the precipitation in the study area used to begin at the end of October. The instrument collected images with the following nominal view angles relative to Earth's surface: 70.5°, 60.0°, 45.6°, and 26.1° forward (cameras Af, Bf, Cf and Df) and aftward (cameras Aa, Ba, Ca and Da) of nadir (camera An, 0°). Each of the nine cameras acquired data, in 7 min at most, in four radiometrically calibrated, geo-rectified and spatially co-registered spectral bands: blue (425–467 nm), green (543–572 nm), red (661–683 nm) and near-infrared (846–886 nm). A more complete description of the MISR instrument can be found in Diner et al. (1998).

Fig. 2 shows the geometry of the six MISR data acquisition. In this investigation, negative (forward cameras) and positive
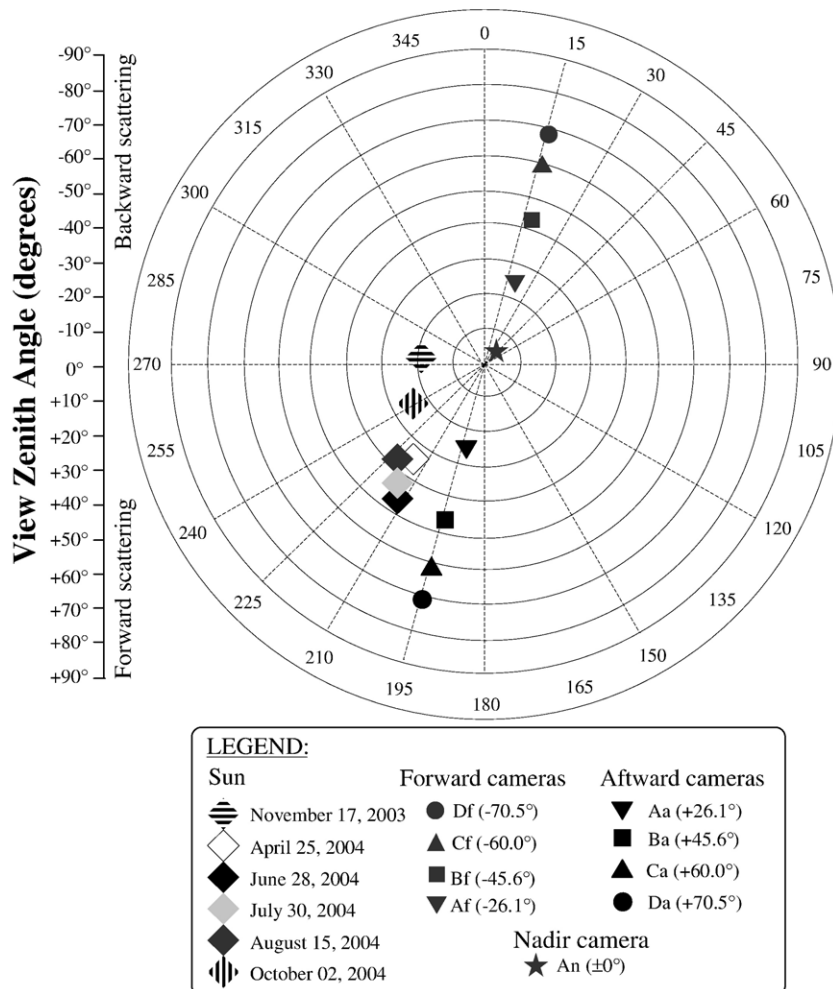

Fig. 2. Geometry of MISR data acquisition for the six dates under analysis.
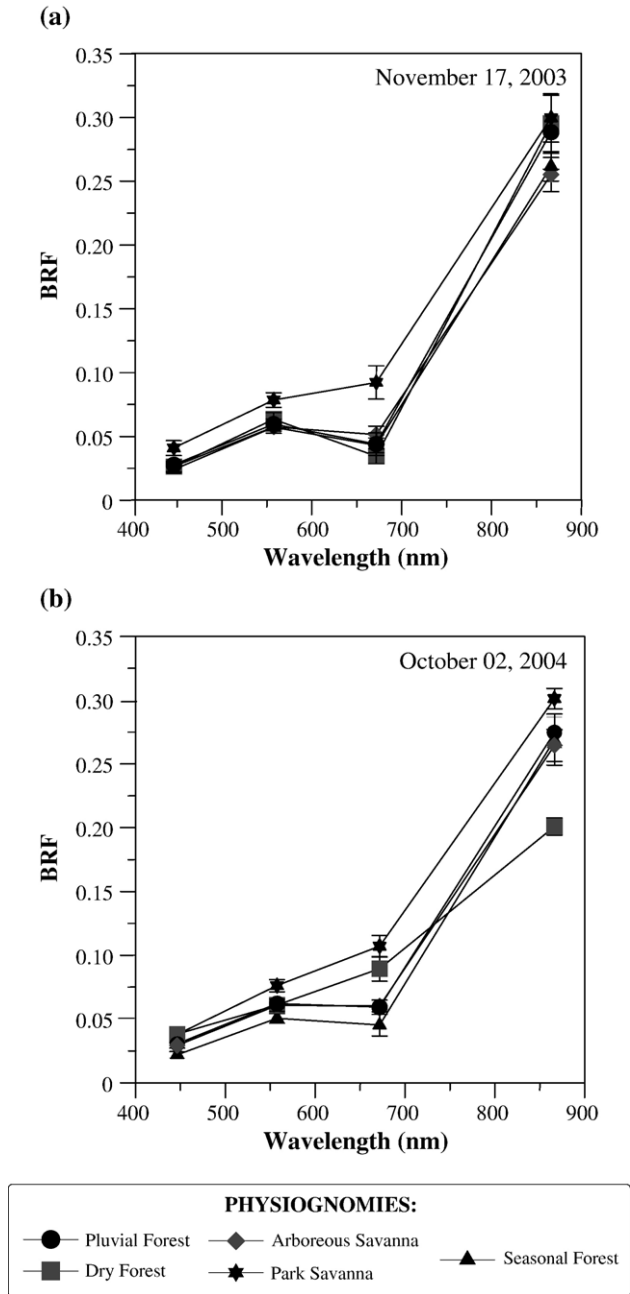
(a)

(b)

Fig. 3. Average Bidirectional Reflectance Factor (BRF) and standard deviation values (10 pixels) of the five physiognomies under study for data acquired at nadir viewing (camera An) on: (a) November 17, 2003; and (b) October 02, 2004. The symbols indicate the centre of the MISR bands.

(aftward cameras) view angles indicate the backward and forward scattering directions, respectively. According to this figure, MISR data from November 17 and October 02 were collected close to the orthogonal plane, whereas data from the remaining dates were acquired close to the solar principal plane.

3.2. Data analysis

The first step in the analysis of the MISR BRF dataset consisted of the selection of pixels in homogeneous areas

representative of the five land cover types under study: Seasonal Forest, Dry Forest, Pluvial Forest, Arboreous Savanna and Park Savanna. This selection was based on the combined analysis of available vegetation maps (e.g., IBGE, 2004), K-Means unsupervised classification results derived from nadir MISR data, and especially on field inspection of potential sites representative of the selected land covers. For each physiognomy, 10 pixels were selected with approximately similar position at each camera image of the different dates. To characterize spectral–angular variations of the physiognomies with seasonality, the BRF data of the four MISR bands, acquired at different view angles (cameras "a" and "f"), were normalized to the nadir response (camera An) at each date and plotted as a function of view and Sun zenith angles. The anisotropic behavior effects of vegetation on the determination of the Normalized Difference Vegetation Index (NDVI) were analyzed. The MISR Level 2 Land Surface products Leaf Area Index (LAI) and Fraction of Photosynthetically Active Radiation (FPAR) (Hu et al., 2003) were also considered in the analysis.

The last step in data analysis was to use the previously selected pixels as training samples to evaluate the seasonality and Sun-view angle effects on the classification of the physiognomies. This step was preceded by the inspection of the spectral distances (Euclidean Distance) between the physiognomies. Differences between the mean distances were evaluated by *t*-tests. The maximum likelihood supervised classification technique (Richards, 1999), which calculated the probability that a given pixel belonged to a specific class with the assumption of a Gaussian distribution for the class data, was then applied at each camera and each date. A reference map showing the spatial distribution of the five physiognomies, elaborated from available vegetation maps (e.g., IBGE, 2004)
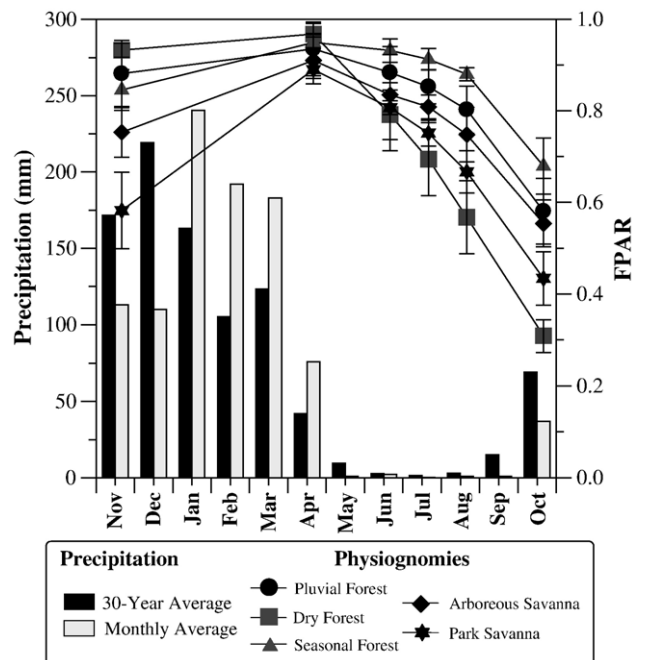

Fig. 4. Seasonal variations in average MISR-derived Photosynthetically Active Radiation (FPAR) and standard deviation values (10 pixels) for the five physiognomies under study as a function of precipitation in the study area.

and updated from fieldwork activities to incorporate land cover changes not previously mapped, was considered as ground truth information. By comparing the classification results with this reference map, classification accuracy (percent pixels correctly classified according to the reference map) was evaluated for each physiognomy, view angle and date of image acquisition (rainy and dry seasons).

Besides the identification of the best view direction to discriminate the physiognomies, the angular contrast information, represented by the Anisotropy Index (ANIX), was also considered in the classification analysis for images collected close to the solar principal plane. According to Sandmeier and Deering (1999), the ANIX is defined as the ratio between the maximum (R_{max}) and minimum (R_{min} BRF values in the principal plane (or defined azimuth plane) per spectral band (wavelength, λ):

$$ANIX(\lambda, \theta_i) = R_{max(\lambda)} / R_{min(\lambda)} \tag{1}$$

where θ is the view angle and i is the illumination direction.

4. Results and discussion

4.1. Seasonal behavior of the savanna physiognomies

Fig. 3 shows the average BRF response at nadir viewing (camera An of MISR) of the five physiognomies under study in

(a)

(b)

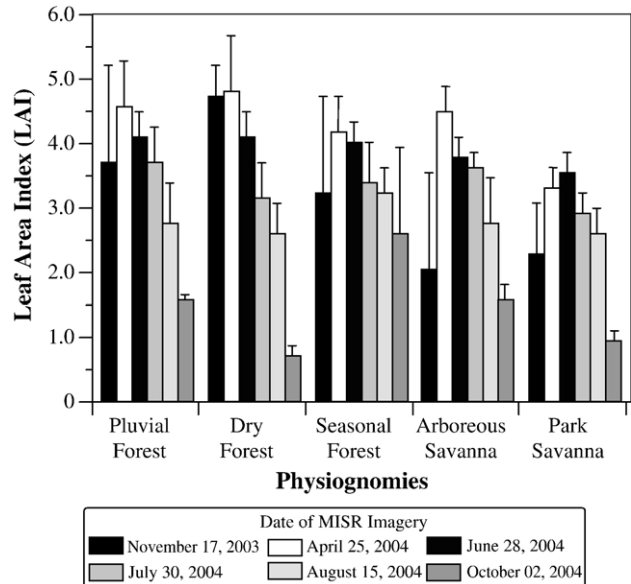Fig. 5. Changes in Dry Forest from the (a) rainy to the (b) dry seasons.

Fig. 6. Seasonal variations in average MISR-derived Leaf Area Index (LAI) values for the five physiognomies under study. Standard deviation bars are indicated.

two distinct dates: November 17, 2003 (Fig. 3a) and October 02, 2004 (Fig. 3b). In the beginning of the rainy season (Fig. 3a), discrimination of the physiognomies was much more difficult than at the end of dry season (Fig. 3b), as indicated by the similarity of the BRF spectra measured in November. In Fig. 3a, the "green-up" of the vegetation (red chlorophyll absorption) due to the beginning of precipitation was apparent for most of the physiognomies, except for Park Savanna which was well discriminated from the other physiognomies due to influence of non-photosynthetic vegetation (dry grasses over the substrate) on its spectral response. The presence of dry grasses over the substrate produced a higher red response for Park Savanna than that verified at the end of the rainy season for this physiognomy (April 25; result not shown). According to Ratana et al. (2005), the rate of "green-up" tends to be slower for herbaceous—than for woody-dominated strata due to the flush in new leaf growth that occurs with the woody plant species. From the rainy (Fig. 3a) to the dry (Fig. 3b) season, an increase in the red reflectance and a decrease in the near-infrared response were observed for most of the physiognomies, especially for Dry Forest due to its almost complete leaf fall.

The relationships between MISR-derived FPAR of the five physiognomies and precipitation values are shown in Fig. 4. As a result of the spectral patterns shown in Fig. 3, some physiognomies presented substantial changes in photosynthetic capacity with seasonality, as indicated by the FPAR values. Changes in the slope of the FPAR profiles calculated from six dates indicate differences in the dynamics of the vegetation response to precipitation. From November to April (rainy season), an overall increase in FPAR was noticed for all physiognomies, which was stronger for Park Savanna especially due to the replacement of the dry grass understore by the green grass cover. From April (rainy season) to the beginning of October (dry season), the precipitation decreased abruptly producing a general decrease in FPAR values for all vegetation types. In Fig. 4, the fastest response to the decrease in precipitation was displayed by Dry Forest that presented an abrupt
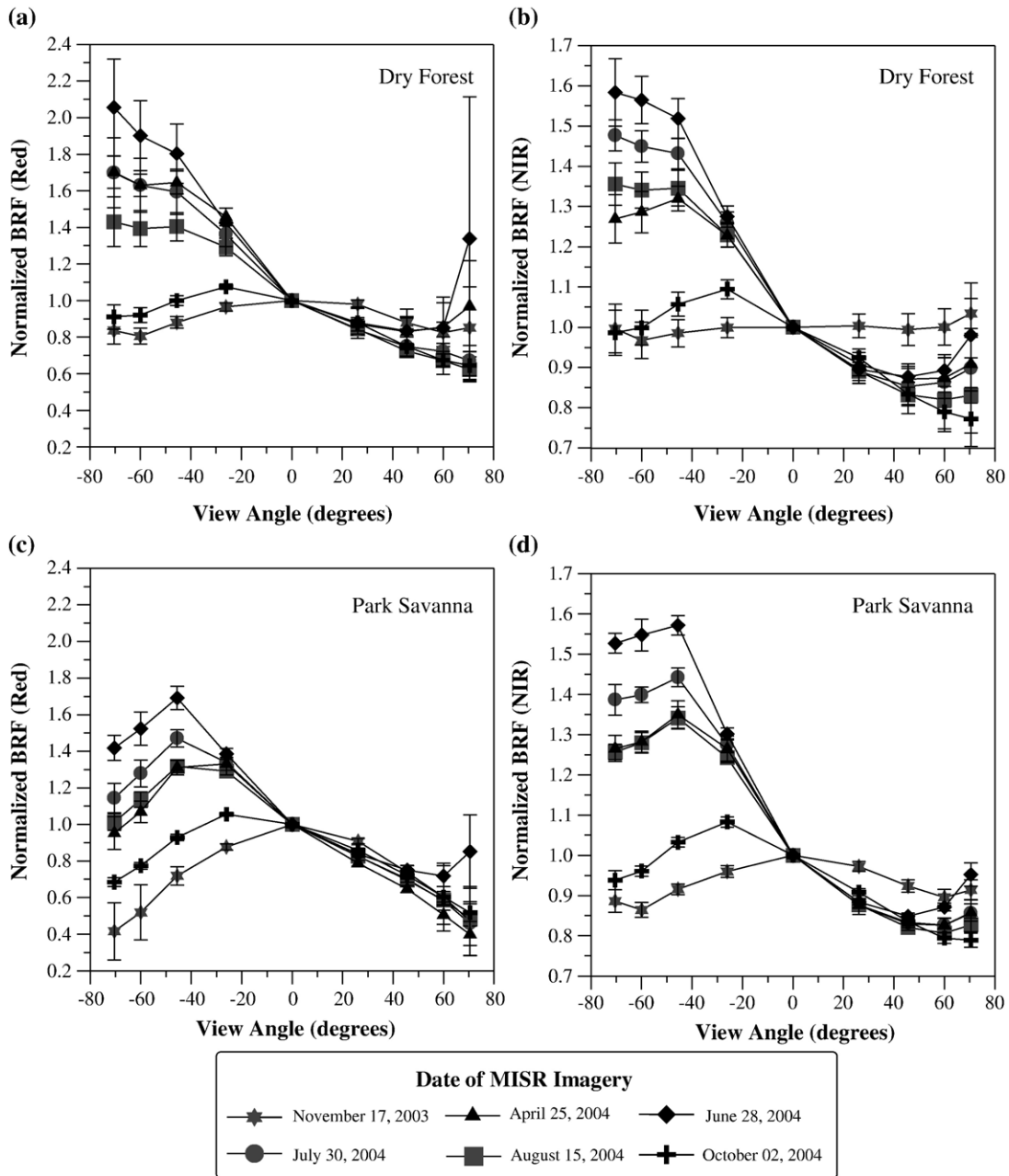
Fig. 7. Seasonal changes in nadir-normalized Bidirectional Reflectance Factor (BRF) angular profiles of the (a, b) Dry Forest and (c, d) Park Savanna. Average and standard deviation values (10 pixels) refer to the red and near-infrared bands of the MISR instrument.

reduction in FPAR values towards the dry season. As illustrated in Fig. 5, the leaves of this physiognomy fell almost completely in the dry season. In Fig. 6, most of the physiognomies showed maximum and minimum MISR-derived LAI values in April (end of the rainy season) and October (end of the dry season), respectively. However, compared with the other physiognomies, Dry Forest showed the strongest reduction in LAI values from the rainy to the dry season.

4.2. Spectral–angular variations of the physiognomies with seasonality

To demonstrate the anisotropic spectral behavior of the physiognomies with seasonality, Fig. 7 shows nadir-normalized

red and near-infrared reflectance values for the Dry Forest (Fig. 7a, b) and Park Savanna (Fig. 7c, d), and six dates of imagery.

As expected, directional effects shown in Fig. 7 were less pronounced for data collected close to the orthogonal plane (November and October) due to the approximately similar proportions of sunlit and shaded canopy components viewed by the sensor. Thus, the anisotropy of the response of both physiognomies increased from November and October (orthogonal plane) up to June (solar principal plane), and from low to high solar zenith angles (Fig. 2). The strongest differences from the nadir response were observed in the backward scattering direction (negative view angles in Fig. 7) with the predominance of illuminated vegetation components for the sensor. The
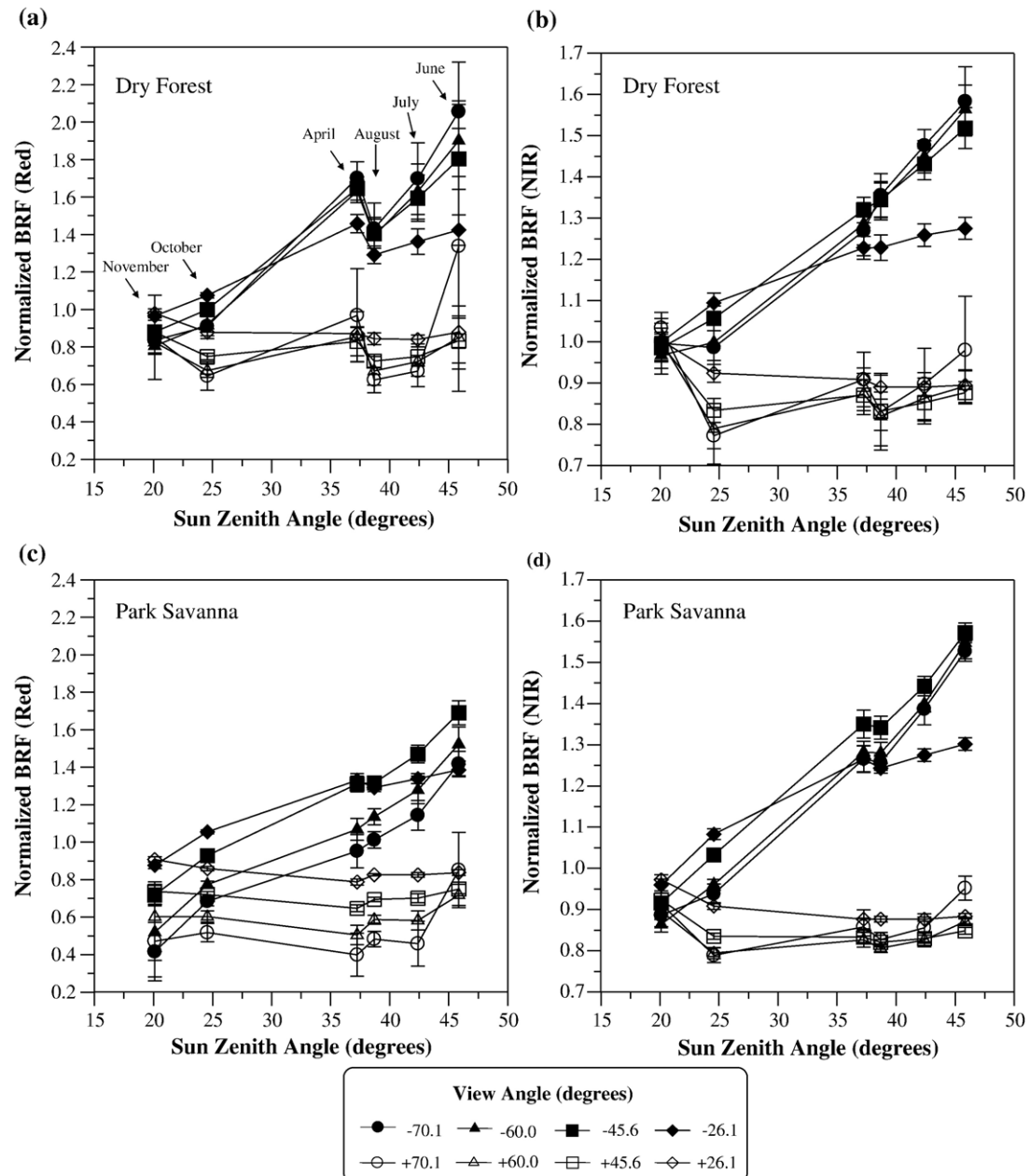
Fig. 8. Variations in nadir-normalized Bidirectional Reflectance Factor (BRF) of the (a, b) Dry Forest and (c, d) Park Savanna as a function of the solar zenith and view angles. Average and standard deviation values (10 pixels) refer to the red and near-infrared bands of the MISR instrument. The month of image acquisition is indicated in (a).

red band (Fig. 7a and c) presented a more anisotropic behavior than the near-infrared band (Fig. 7b and d), as indicated by the wider range of normalized BRF data in the backward scattering direction. This result is in agreement with that obtained by Sandmeier and Deering (1999). According to them, directional effects are particularly strong in spectral regions of high absorbance such as the red chlorophyll interval. On the other hand, they are less pronounced in the near-infrared due to the predominance of multiple scattering processes that reduce the spectral contrast between shadowed and illuminated canopy components (Sandmeier et al., 1998).

In the backward scattering direction and for data collected in the solar principal plane, Dry Forest (Fig. 7a and b) presented a

more anisotropic angular response than Park Savanna (Fig. 7c and d). However, the contrary was verified for images collected in the orthogonal plane (November and October) at the same viewing direction (negative view angles), especially for the red band. The directions of maximum reflectance were better defined in the principal plane for Park Savanna than for Dry Forest. In Fig. 7c and d, maximum backscattering was observed at view angles ranging from the camera Af (−26.1°) to the camera Bf (−45.6°). The hot spot effect, which comprised the antisolar direction of maximum reflectance and minimum shadowing, was evident in the angular profiles of Park Savanna (Fig. 7c and d) for data acquired with large Sun zenith angles (July and June) at view angle of −45.6°.

Results obtained for the other physiognomies (not shown) followed the same general trend displayed by the angular profiles of Fig. 7 but with different degrees of anisotropy. Such results enhanced the land cover type dependence of the directional effects in the savanna environment. These effects became complex with seasonality due to variations in Sun zenith angles and in proportions of green and non-photosynthetic vegetation (overstore and understore), and to the resultant modifications in vegetation structural characteristics.

As illustrated in Fig. 8, the anisotropy shown in Fig. 7 changes significantly with the Sun zenith angle. Thus, the angular profiles of the savanna physiognomies (Dry forest and Park Savanna) are not conserved over time, especially in the backward scattering direction (close symbols in Fig. 8). In fact, such profiles may also vary in some extent with latitude/longitude in a given scene. In Fig. 8, for a given view angle in the backward scattering direction, directional effects were stronger with increasing Sun zenith angles, or from November (beginning of the rainy season) and October (end of the dry season) to June (dry season). The influence of the seasonality on the shape of the Dry Forest profiles (Fig. 8a) can be noticed on April (end of the rainy season).

Fig. 9 indicates that the directional effects of Fig. 7 are not completely removed after NDVI determination. In Fig. 9a, in comparison with nadir viewing and for data collected close to the principal plane with large Sun zenith angles (April, June, July and August), Dry Forest presented lower NDVI values in the backward scattering direction (negative view angles) due to an increase in red reflectance towards extreme viewing. It also displayed higher NDVI values in the forward scattering direction (positive view angles) due to a decrease in red response towards large view angles. In comparison with nadir viewing and for data collected in the orthogonal plane with low Sun zenith angle (November and October), Dry Forest showed higher NDVI values in both scattering directions (Fig. 9a) especially due to a decrease in red reflectance with increasing view angles.

In Fig. 9b, Park Savanna exhibited a different pattern from Dry Forest for data collected in the principal plane (April, June, July and August). In comparison with nadir viewing, NDVI values first decreased in the backward scattering direction up to view angles of maximum reflectance in the red interval ($-26.1°$ and $-45.6°$ in Fig. 7c). Then, they increased as a function of the decrease in red reflectance with large view angles.

In Figs. 7, 8 and 9, standard deviation values tend to increase from nadir to extreme view angles. This trend may be associated with the uncertainties of the MISR BRF data. The causes of uncertainties were discussed by Hu et al. (2003) and may include factors such as the removal of atmospheric effects at extreme viewing.

4.3. Classification of physiognomies with view angle and seasonality

The effects of seasonality and viewing geometry on the discrimination of the physiognomies are illustrated in Fig. 10. Fig. 10a shows variations in Euclidean Distance values for the

(a)

(b)

Date of MISR Imagery
— November 17, 2003   — April 25, 2004   — June 28, 2004
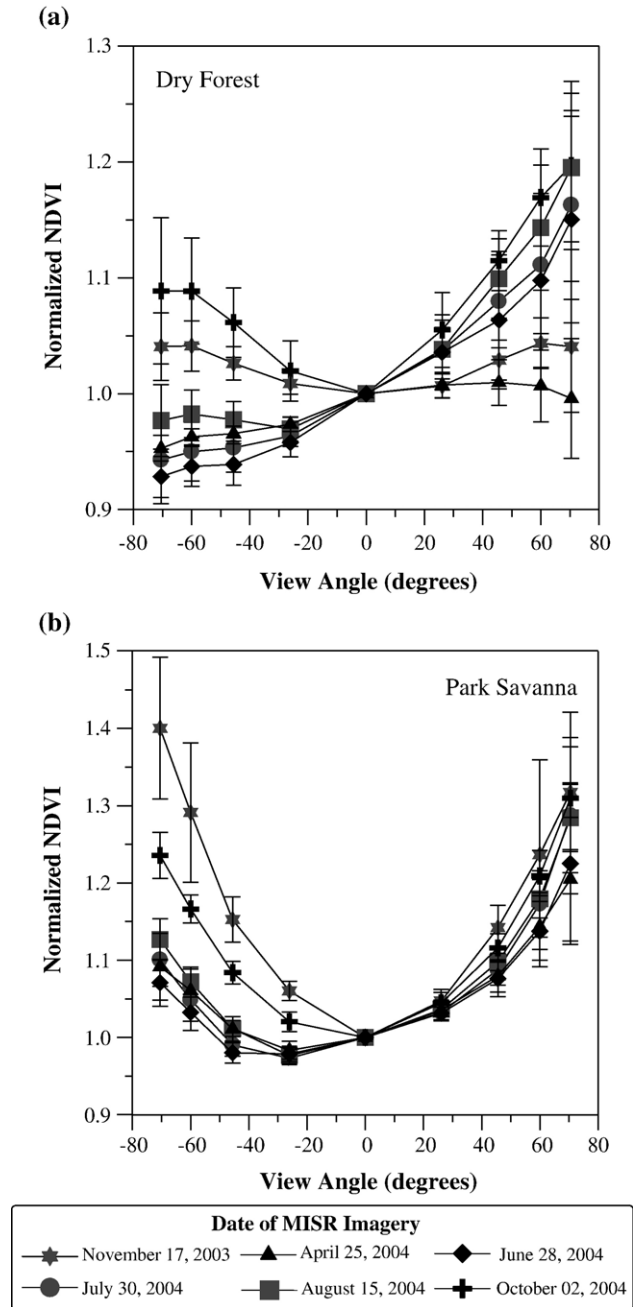— July 30, 2004   — August 15, 2004   — October 02, 2004

Fig. 9. Seasonal variations in nadir-normalized NDVI angular profiles of the (a) Dry Forest and (b) Park Savanna. Standard deviation values (10 pixels) are indicated.

discrimination between Arboreous Savanna and Park Savanna whereas Fig. 10b presents the results for the distinction between Dry Forest and Seasonal Forest. In each figure, average values above the horizontal dashed line are statistically different (t-test; significance level of 0.05) from the lowest mean distance (camera Da; June and April, respectively).

In Fig. 10a, the best results (the largest Euclidean Distance values) for the discrimination between Arboreous Savanna and Park Savanna were obtained for images collected in the beginning of the rainy season (November 17, 2003) and at the end of the dry season (October 02, 2004). In the beginning of the rainy season,
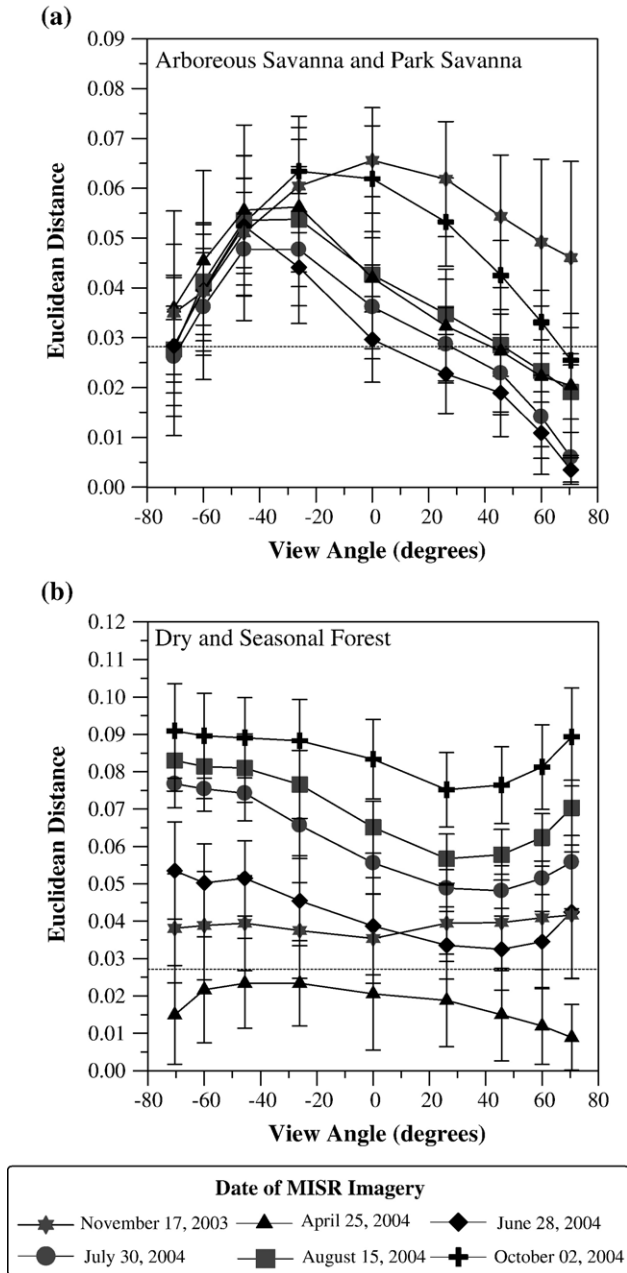
(a)

(b)

Fig. 10. Variations in Euclidean Distance values (average and standard deviation values for 10 pixels) as a function of seasonality and view angle for the discrimination between (a) Arboreous Savanna and Park Savanna; and (b) Dry Forest and Seasonal Forest. Values above the horizontal dashed line are statistically different (*t*-test; significance level of 0.05) from the lowest mean distance (camera Da) in each figure.

great amounts of non-photosynthetic vegetation over the substrate viewed by the sensor facilitated the discrimination of Park Savanna from the other physiognomies, as indicated also by the BRF spectra of Fig. 3a. In Fig. 10a, discrimination improved from the forward (positive view angles) to the backward (negative view angles) scattering directions up to view angles that produced the maximum backscattering.

In Fig. 10b, discrimination between Dry Forest and Seasonal Forest improved from the rainy (November 17, 2003 and April

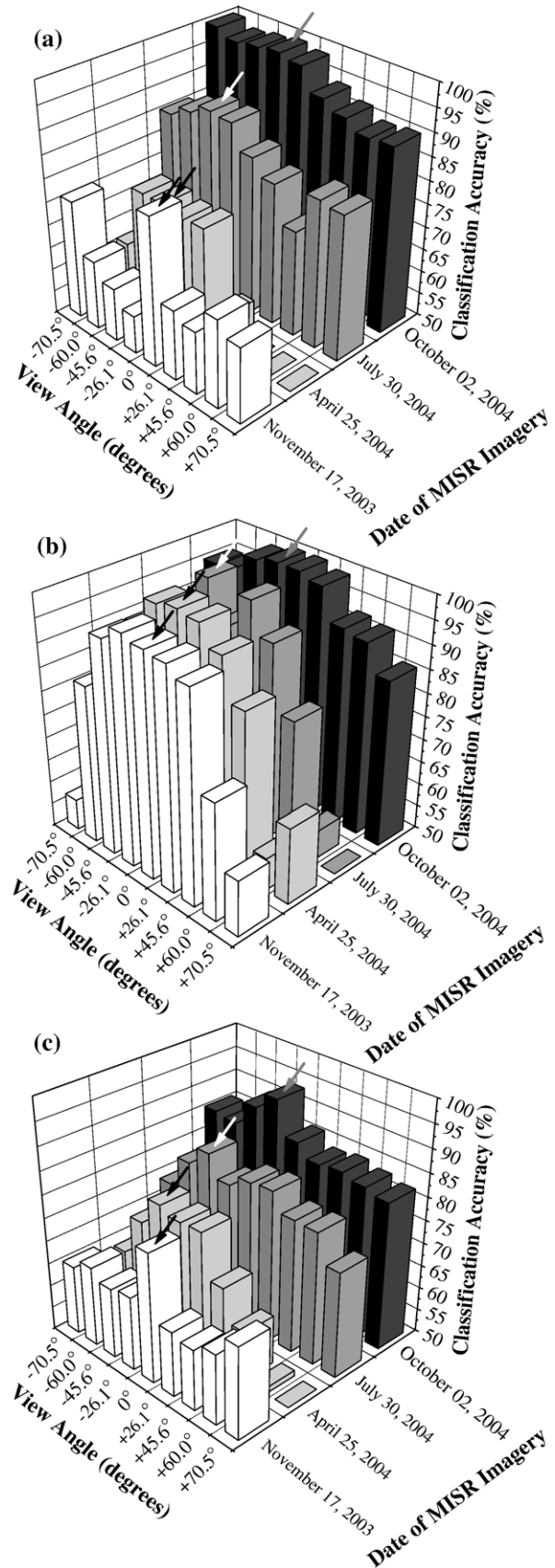**(a)**

(b)

(c)

Fig. 11. Variations in classification accuracy values with seasonality and view angles for (a) Dry Forest; (b) Park Savanna; and (c) all physiognomies. View angles with the best results of classification accuracy are indicated by arrows.

25, 2004) to the dry season (October 02, 2004). This result is consistent with that presented in Fig. 3 that shows greater separability between the two physiognomies on October 02 (Fig. 3b) than on November 17 (Fig. 3a). In general, better results were obtained in the backward scattering direction than in the forward scattering direction, especially for images collected in the principal plane. All dates except April presented statistically different mean values.

Fig. 11 shows classification accuracy results as a function of the seasonality and view angles for Dry Forest (Fig. 11a), Park Savanna (Fig. 11b), and all physiognomies (Fig. 11c). To facilitate graphic representation, results were presented only for four of the six dates of MISR image acquisition.

For Dry Forest (Fig. 11a), classification accuracy improved from the rainy (November and April) to the dry (October) season, and from the forward (positive view angles) to the backward (negative view angles) scattering direction. The best view angles for classification purposes, indicated by arrows, ranged from 0° (nadir) to −45.6°, and corresponded to viewing directions of maximum backscattering of this vegetation type at each date. For Park Savanna (Fig. 11b), the largest classification accuracy values were obtained also at view angles close to nadir. However, the best results were verified in the beginning of the rainy season (November) and at the end of the dry season (October) due to the spectral influence of the dry grass understore that facilitated its discrimination from the other physiognomies, as explained before for Fig. 3. Results for all physiognomies under analysis (Fig. 11c) showed a similar trend to Fig. 11a. In Fig. 11c, an improvement of the overall classification accuracy results was observed from the rainy (e.g., 77% at nadir on April 25) to the dry (e.g., 87% at nadir on October 02) season, and from the forward (e.g., 82% at +70.5° view angle on October 02) to the backward (e.g., 93% at −26.1° view angle on October 02) scattering direction.

When the angular contrast information was considered in the analysis, as indicated by the classification of ANIX images acquired in the principal plane, a general decrease in classification accuracy was observed for the savanna physiognomies that presented values lower than 60%. For example, classification of ANIX MISR data from July, derived from the −45.6° backward (hot spot or maximum reflectance in Fig. 7c and d) and +45.6° forward (minimum reflectance) scattering directions, produced overall accuracy results of 52% against 84% at −45.6° view angle. According to Sandmeier and Deering (1999), in comparison with nadir data, the use of ANIX data may increase or decrease classification accuracy depending on the land cover type under study.

5. Conclusions

Results demonstrate that the surface anisotropy signatures of the savanna physiognomies are not unique and may vary with view and Sun zenith angles and seasonality. Directional effects increased from MISR data collected in the orthogonal plane (November and October) to those acquired in the solar principal plane (April, August, July and June), or with increasing Sun zenith angles. It occurred because of the approximately similar proportions of sunlit and shaded canopy components viewed by the sensor in the orthogonal plane. The directional effects were

stronger for large Sun zenith angles and were also affected by seasonality due to differences in the dynamics of the vegetation response to precipitation, as indicated by FPAR and LAI values. For example, Dry Forest presented a fast rate of "green-up" (red chlorophyll absorption) in the beginning of the rainy season and abrupt changes in LAI values early in the dry season. As a result, a substantial change in the slope of the FPAR profile was observed for this physiognomy from the rainy to the dry season.

In relation to the nadir response, the strongest anisotropy was observed in the backward scattering direction and in the red band. In the backward scattering direction and for data collected with large Sun zenith angles in the solar principal plane, Dry Forest presented a more anisotropic angular response than Park Savanna but the opposite pattern was verified for images collected with low Sun zenith angles in the orthogonal plane at the same viewing direction, especially for the red band. The land cover type dependence of such directional effects was also observed after NDVI determination.

The effects of Sun-view geometry and seasonality affected the discrimination of the physiognomies. In general, classification accuracy of vegetation improved from the rainy (November and April) to the dry (October) season. The exception was Park Savanna that was also well discriminated from the other physiognomies in the beginning of the rainy season (November) because of the spectral influence of non-photosynthetic vegetation (dry herbaceous understore) that produced a red reflectance increase. In general, classification accuracy of the physiognomies improved also from the forward to the backward scattering direction, or from the transition of shadowed to dominant sunlit canopy components viewed by the sensor. The best view angles for classification purposes ranged from 0° (nadir) to −45.6°, and were associated with viewing directions of maximum backscattering of the physiognomies at the different dates. In comparison with single view direction results, the use of ANIX images produced a general decrease in classification accuracy values.

References

Abuelgasim, A. A., Gopal, S., Irons, J. R., & Strahler, A. H. (1996). Classification of ASAS multiangle and multispectral measurements using artificial neural networks. *Remote Sensing of Environment*, *57*(2), 79−87.

Asner, G. P., Braswell, B. H., Schimel, D. S., & Wessman, C. A. (1998). Ecological research needs from multiangle remote sensing. *Remote Sensing of Environment*, *63*(2), 155−165.

Braswell, B. H., Hagen, S. C., Frolking, S. E., & Salas, W. A. (2003). A multivariable approach for mapping sub-pixel land cover distributions using MISR and MODIS: Application in the Brazilian Amazon region. *Remote Sensing of Environment*, 87(2–3), 243−256.

Diner, D. J., Asner, G. P., Davies, R., Knyazikhin, Y., Muller, J. P., Nolin, A. W., et al. (1999). New directions in earth observing: Scientific applications of multiangle remote sensing. *Bulletin of the American Meteorological Society*, 80(11), 2209−2228.

Diner, D. J., Beckert, J. C., Reilly, T. H., Bruegge, C. J., Conel, J. E., Kahn, R. A., et al. (1998). Multi-angle Imaging SpectroRadiometer (MISR): Instrument description and experiment overview. *IEEE Transactions on Geoscience and Remote Sensing*, 36(4), 1072−1087.

Diner, D. J., Braswell, B. H., Davies, R., Gobron, N., Hu, J. N., Jin, Y. F., et al. (2005). The value of multiangle measurements for retrieving structurally and radiatively consistent properties of clouds, aerosols, and surfaces. *Remote Sensing of Environment*, 97(4), 495−518.

Eiten, G. (1982). Brazilian savannas. *Ecological Studies*, 42, 25−47.

Ferreira, L. G., & Huete, A. R. (2004). Assessing the seasonal dynamics of the Brazilian Cerrado vegetation through the use of spectral vegetation indices. *International Journal of Remote Sensing*, 25(10), 1837−1860.

Ferreira, L. G., Yoshioka, H., Huete, A., & Sano, E. E. (2004). Optical characterization of the Brazilian savanna physiognomies for improved land cover monitoring of the Cerrado biome: Preliminary assessments from an airborne campaign over an LBA core site. *Journal of Arid Environments*, 56(3), 425−447.

Galvão, L. S., Ponzoni, F. J., Epiphanio, J. C. N., Rudorff, B. F. T., & Formaggio, A. R. (2004). Sun and view angle effects on NDVI determination of land cover types in the Brazilian Amazon region with hyperspectral data. *International Journal of Remote Sensing*, 25(10), 1861−1879.

Gillon, D. (1983). The fire problem in tropical savannas. In F. Bourlière (Ed.), *Tropical savanna* (pp. 617−641). New York: Elsevier.

Gobron, N., Pinty, B., Verstraete, M. M., Widlowski, J., & Diner, D. J. (2002). Uniqueness of multiangular measurements - Part II: Joint retrieval of vegetation structure and photosynthetic activity from MISR. *IEEE Transactions on Geoscience and Remote Sensing*, 40(7), 1574−1592.

Hansen, M. C., DeFries, R., Townshend, J. R. G., Sohlberg, R., Dimiceli, C., & Carroll, M. (2002). Towards an operational MODIS continuous field of percent tree cover algorithm: Examples using AVHRR and MODIS data. *Remote Sensing of Environment*, 83(1–2), 303−319.

Hu, J. N., Tan, B., Shabanov, N., Crean, K. A., Martonchik, J. V., Diner, D. J., et al. (2003). Performance of the MISR LAI and FPAR algorithm: A case study in Africa. *Remote Sensing of Environment*, 88(3), 324−340.

IBGE (1992). *Manual técnico da vegetação do Brasil.* Rio de Janeiro: Instituto Brasileiro de Geografia e Estatística (IBGE).

IBGE (2004). *Mapa de vegetação do Brasil.* Rio de Janeiro: Instituto Brasileiro de Geografia e Estatística (IBGE).

Jepson, W. (2005). A disappearing biome? Reconsidering land cover change in the Brazilian savanna. *Geographical Journal*, 171(2), 99−111.

Kimes, D. S., Harrison, P. A., & Harrison, P. R. (1994). Extension of off-nadir view angles for directional sensor systems. *Remote Sensing of Environment*, 50(3), 201−211.

Kimes, D. S., Holben, B. N., Tucker, C. J., & Newcomb, W. W. (1984). Optimal directional view angles for remote sensing missions. *International Journal of Remote Sensing*, 5(6), 887−908.

Leroy, M., & Roujean, J. (1994). Sun and view angle corrections on reflectances derived from NOAA/AVHRR data. *IEEE Transactions on Geoscience and Remote Sensing*, 32(3), 684−697.

Lotsch, A., Tian, Y., Friedl, M. A., & Myneni, R. B. (2003). Land cover mapping in support of LAI and FPAR retrievals from EOS-MODIS and MISR: Classification methods and sensitivities to errors. *International Journal of Remote Sensing*, 24(10), 1997−2016.

Nolin, A. W. (2004). Towards the retrieval of forest cover density over snow from the Multi-angle Imaging SpectroRadiometer (MISR). *Hydrological Processes*, 18(18), 3623−3636.

Oliveira-Filho, A. T., & Ratter, J. (2002). Vegetation physiognomies and woody flora of the Cerrado biome. In P. S. Oliveira & T.J. Marques (Eds.), *The Cerrados of Brazil: Ecology and natural history of a neotropical savanna* (pp. 91−120). New York: Columbia University Press.

Ratana, P., Huete, A. R., & Ferreira, L. (2005). Analysis of Cerrado physiognomies and conversion in the MODIS seasonal–temporal domain. *Earth Interactions*, 9(3), 1−22.

Ribeiro, J. F., & Walter, T. M. B. (1998). Fitofisionomias do bioma Cerrado. In S. M. Sano & S.P. Almeida (Eds.), *Cerrado: Ambiente e Flora* (pp. 89−152). Brasília: Empresa Brasileira de Pesquisa Agropecuária (Embrapa).

Richards, J. A. (1999). *Remote sensing digital image analysis.* Berlin: Springer–Verlag 240 pp.

Sandmeier, St., & Deering, D. W. (1999). Structure analysis and classification of Boreal forests using airborne hyperspectral BRDF data from ASAS. *Remote Sensing of Environment*, 69(3), 281−295.

Sandmeier, St., Müller, C., Hosgood, B., & Andreoli, G. (1998). Physical mechanisms in hyperspectral BRDF data of grass and watercress. *Remote Sensing of Environment*, 66(2), 222−233.

Sano, E. E., Barcellos, A. O., & Bezerra, H. S. (2001). Assessing the spatial distribution of cultivated pastures in the Brazilian savanna. *Pasturas Tropicales*, 23(3), 2−15.

Sano, E. E., Ferreira, L. G., & Huete, A. R. (2005). Synthetic Aperture Radar (L-band) and optical vegetation indices for discriminating the Brazilian savanna physiognomies: A comparative analysis. *Earth Interactions*, 9(15), 1−15.

Sarmiento, G. (1983). The savannas of tropical America. In F. Bourlière (Ed.), *Tropical savannas* (pp. 245−288). New York: Elsevier.

Silva, J. M. C., & Bates, J. M. (2002). Biogeographic patterns and conservation in the South American Cerrado: A tropical savanna hotspot. *Bioscience*, 52(3), 225−233.

Verbrugghe, M., & Cierniewski, J. (1995). Effects of Sun and view geometries on cotton bidirectional reflectance. *Remote Sensing of Environment*, 54(3), 189−197.

Xavier, A. S., & Galvão, L. S. (2005). View angle effects on the discrimination of selected Amazonian land cover types from a principal-component analysis of MISR spectra. *International Journal of Remote Sensing*, 26(17), 3797−3811.

Walther-Shea, E. A., Privette, J., Cornell, D., Mesarch, M. A., & Hays, C. J. (1997). Relations between directional spectral vegetation indices and leaf area and absorbed radiation in alfalfa. *Remote Sensing of Environment*, 61(1), 162−177.

Zhang, Y., Tian, Y., Myneni, R. B., Knyazikhin, Y., & Woodcock, C. E. (2002). Assessing the information content of multiangle satellite data for mapping biomes: I. statistical analyses. *Remote Sensing of Environment*, 80(3), 418−434.